Thin-Walled Structures 167 (2021) 108200

Contents lists available at ScienceDirect

Thin-Walled Structures

journal homepage: www.elsevier.com/locate/tws

Full length article

Cut-out resonators for tuned vibration suppression of plates

Sih-Ling Yeh [a], Ryan L. Harne [b,*]

[a] Department of Mechanical and Aerospace Engineering, The Ohio State University, Columbus, OH 43210, USA
[b] Department of Mechanical Engineering, The Pennsylvania State University, University Park, PA 16802, USA

ARTICLE INFO

Keywords:
Plates
Vibration
Resonators
Coupling mechanisms

ABSTRACT

This research investigates a concept for cut-out resonators that exploit a small area of active mass of a host plate structure for sake of tuned, low frequency vibration attenuation. Integrated computational and experimental studies reveal that embedding the resonators at locations offering high bending moment gradient and arranging the central resonator beam along a nodal line of bending moment best excite the first resonator eigenmode for targeted vibration suppression. These results are independent of plate boundary conditions and do not require periodic resonators to achieve notable vibration suppression outcomes. These design concepts may guide the development of resonators for vibration absorption of plates with arbitrary boundary conditions.

1. Introduction

The pursuit for low frequency vibration attenuation of plates has flourished in automotive, aerospace, or civil engineering applications. The mechanisms of tuned mass damping and bandgaps are commonly used to mitigate undesired vibrations of plates. The classic tuned mass damper (TMD) is essentially a mass connected to the host structure by a parallel combination of spring and damper [1]. Vibration energy is mitigated by reactive inertial force from the TMD against the exciting force, leading to a passive elimination of vibration over a tuned frequency range. Researchers have investigated methods to improve the effectiveness [2–6] and robustness [5,6] of TMDs. For example, the studies on single TMDs applied to one degree-of-freedom (1-DOF) host structures indicate that interfacing the TMD damper element with a ground is more effective than when the TMD damper interfaces directly with the host structure [2,7]. The addition of elastic springs in parallel to grounded dampers provides TMDs still greater effectiveness by offering a complex impedance path to the ground by which to attenuate host structure vibration [3,8]. Increasing the number of TMDs may improve the vibration absorption capabilities [4,5,9,10]. Li and Ni [6] report that the optimal non-uniform distribution of TMDs delivers greater vibration attenuation than uniform distributions of optimized TMDs. Zuo [5] finds that serially interfaced TMDs are more effective and robust than parallel connected TMDs. Moreover, Igusa and Xu [10] point out the operating frequency range of a TMD is proportional to the square root of mass ratio. Extending from 1-DOF host structures to continuous structures, studies discuss how TMDs suppress the vibrations of plates [11,12]. Cheung and Wong [11] suggest that an optimal TMD for a targeted mode of plate vibration has a high mass ratio. Although the effectiveness and robustness may be improved by modifying the arrangements of mass, spring, and damper elements, a large ratio of TMD mass to structure mass is required to obtain substantial vibration suppression [9].

For a periodic array of 1-DOF TMDs on a plate, bandgaps for wave propagation are developed by introducing the concept of negative effective mass [13–15]. Standing and traveling waves at the frequencies within bandgap are inhibited from propagating through the periodic structures. Sugino et al. [16] report that the normalized bandgap bandwidth is $\sqrt{1+\mu}-1$, where μ is the mass ratio between the TMDs and host structure. Researchers also explore 2-DOF TMDs [17,18] and multiple DOF (MDOF) resonators in periodic arrays to extend the functionality of wave attenuating bandgaps. Here, the MDOF resonators may be pillars [19–21], rubber inclusions [22], interconnected beams [23–25], and membrane/plate type resonators [26,27]. For the MDOF resonators applied to plates, bandgaps are induced by destructive interference between Bragg scattered waves. Compared with 1-DOF TMDs, the number of bandgaps that MDOF resonators may produce lead to multiple bandgaps tailored by the arrangement of the resonators [28,29]. Yet, the bandgaps of MDOF resonators are often effective in mid to high frequency range, while many plate vibration challenges are in the low frequency range.

To overcome the limitation of relying on large added mass ratios to achieve large attenuation of low frequency elastic waves and mechanical vibrations, researchers have designed tuned inerter dampers [30–32], piezoelectric patches [33,34] and lightweight resonators [35–37]. Using tuned inerter dampers, vibration isolation can be achieved by a small amount of added mass compared to classical TMDs. For piezoelectric patches, Toftekær et al. [33] proposed patches with piezoelectric shunt damping for plate vibration suppression using only 5% mass ratio

* Corresponding author.
E-mail address: ryanharne@psu.edu (R.L. Harne).

https://doi.org/10.1016/j.tws.2021.108200
Received 3 February 2021; Received in revised form 27 May 2021; Accepted 15 July 2021
Available online xxxx
0263-8231/

and 4% surface area coverage of the host plate, but this design requires an external connection to a shunt circuit. Sun et al. [35] presented periodic grid frames filled with rubber membranes to attenuate plate vibration at low frequencies. For this periodic structure, the mass ratio may be as low as 6%, although the area coverage of the resonators constitutes around 50% of the host plate area. Recently, the authors developed a lightweight elastomeric half cylindrical resonator for vibration suppression of an aluminum panel [37]. The peak amplitude of plate vibration around 140 Hz was reduced by 8 dB by applying only four resonators on the plate accounting for a mass ratio of just 3.3% and the area coverage of 1.7% of the plate surface. These functionalities were achieved by exploiting the multimodal nature of the locally resonant elastomeric attachments [37]. Rather than devise resonators from add-on elements, researchers have investigated resonators realized by cut-outs from a host structure [38–40]. Yet, to date the operating frequency ranges of such cut-out resonators are high considering structure-borne vibrations, such as in the kHz range, and the cut-out resonators require a large area coverage. Ulz and Semercigil [41] studied the dynamic responses of a clamped plate with a single cut-out resonator and discuss the possibility to employ such resonators for low frequency vibration attenuation. While an important step to address the outstanding needs for effective lightweight and minimally intrusive application of vibration absorbers to continuous structures, the discussion of resonator design and positioning is limited in terms of frequency responses for achieving vibration control [41].

This research explores an approach for cut-out resonators in non-load-bearing plates that provides vibration suppression at low frequencies without excessive use of the plate surface area. By examining the resonant mechanisms of the cut-outs, the linear modes are exploited to capitalize on the cut-out resonator positioning for multi-mode vibration attenuation. The following sections of this report detail computational and experimental efforts undertaken to characterize the modal nature of the resonators and to analyze the vibration attenuation mechanisms of the resonators integrated with a host plate structure. The findings and implications from the insights of this research are summarized in the final section.

2. Modal characteristics of the cut-out resonators

The host structure with cut-out resonators considered in this research is schematically shown in Fig. 1(a). The host structure is a 3 mm thick acrylic rectangular plate. In order to avoid reducing necessary mechanical performance of the plates via the cut-out inclusions, we envision that the host structure plate is involved in a non-load-bearing application, such as serving as a cover over other mechanical or structural members, yet still essential in the vibration transmission scenario. The cut-out resonator is created by removal of material from the host structure, to realize a slender body interfaced with the host structure by small beams of width t. The cut-out resonator mass elements constitute two triangles on either side of the central beam that interfaces with the host structure. The geometric notations of the resonator are given in the inset of Fig. 1(a). The cut-out resonator has the same thickness h as the host plate. Hereafter, the term cut-out resonators refers to the resonator structures designed and shown in Fig. 1(a).

To understand the modal characteristics of the cut-out resonator, finite element (FE) based modal analyses (COMSOL Multiphysics, Stockholm, Sweden) are conducted. An FE resonator model of the slender beam with two triangular mass elements is created using quad shell elements due to the small rotations that the resonator undergoes. A solid model of the resonators was also considered for comparison and convergence purposes, and the results of the shell approximation were found to be in good agreement with the solid model for all of the modal and resonant frequencies of interest in this report. Both ends of the cut-out resonator beam are fixed. The linear elastic material properties of the acrylic are: Young's modulus 3.2 GPa, density 1190 kg/m^3, Poisson's ratio 0.35, and structural loss factor 0.08. The structural loss factor is estimated by the average of the experimental modal loss factors of the lowest three order modes of the clamped acrylic plate. The modal loss factors at the lowest three order modes are calculated by the half-power bandwidth method in the experimental frequency responses.

Fig. 1(b) present the first resonator eigenfrequencies for four sizes of the mass elements as a function of the beam width. The insets of Fig. 1(b) exemplify the relative sizes of the resonator masses. The insets also highlight the total displacement of the first eigenmode for the respective resonator. The total displacement is the square root of the sum of square of x-, y-, and z-displacement components. As shown in the first eigenmode shape in the inset, the resonator deforms by rocking back-and-forth, out-of-plane with a twist around the central slender beam. The mode shape implies that the resonator can be triggered by the out-of-plane forces applying on the two triangular masses.

As seen in Fig. 1(a), the base length and height of the triangular mass are dimensioned according to $c - 2g$ and $0.5d - g$, respectively, where c is the cut-out width, d is the cut-out length, and g is the gap between the cut-out and the resonator mass. Four resonators are considered in Fig. 1(b). The triangular mass base lengths and heights for resonator R1 are 10 mm and 10 mm, 20 mm and 20 mm for R2, 20 mm and 30 mm for R3, and 30 mm and 20 mm for R4. In Fig. 1(b), the first resonator eigenfrequency increases for decrease in the triangular mass area for a constant width of the slender beam that interfaces the resonator to the host plate. This result is intuitive by an understanding of natural frequency inverse proportionality to change of the mass. Resonators R3 and R4 have the same overall mass extended from the central slender beam, yet the first eigenfrequency of R3 is less than that of R4 in Fig. 1(b). The greater length of the triangular masses of resonator R3 leads to a greater radius of gyration leads and thus a greater moment of inertia about the central slender beam. As a result, the rotational eigenfrequency of the resonator is reduced. Using the same weight and cut-out area of the resonator, a cut-out with increased moment of inertia around the central slender beam reduces the first eigenfrequency. In addition to the first eigenfrequency tailored by the length of the triangular masses, the other crucial parameter is beam width of the central slender beam. For the four resonators in Fig. 1(b), the first eigenfrequency monotonically increases with the increasing beam width for the same cut-out area of the resonator. This is because the greater beam width results in a stiffer beam and thus increasing the twisting eigenfrequency of the resonator.

3. Experimental and finite element investigation methods

The experimental system is a 3 mm thick, clamped acrylic plate that includes cut-out resonators, as shown in Fig. 2(a). A laser cutter (Epilog, Mini/Helix 8000, Golden, CO, USA) is used to cut the exterior shape of the acrylic plate, the mounting holes in the plate for clamping, as well as potential cut-out resonators employed. The area of the acrylic plate inside the clamped edges is 203.2 mm by 241.3 mm. The clamping frame is placed on foam supports to minimize coupling between dynamics associated with the clamping frame itself and the acrylic plate of interest.

To examine the vibration responses of the clamped plate with and without cut-out resonators, an impact hammer strikes the acrylic plate with a roving accelerometer positioned on the plate surface. The impact force is generated by a modal hammer (PCB 086C01) delivered to the position represented by the green triangle marker in Fig. 2(a). The impact position is selected since it avoids displacement nodal lines of the three lowest order plate modes. The accelerometer (PCB 352A24) is mounted on the rear of the plate with respect to the impact force. To measure the global response of the plate, the 25 periodically distributed measurement positions are used, shown as the red circle markers in Fig. 2(a). When using plates with a cut-out resonator for which the resonator overlaps with the accelerometer position, no data is acquired for that position, such as the central plate position in Fig. 2(a).

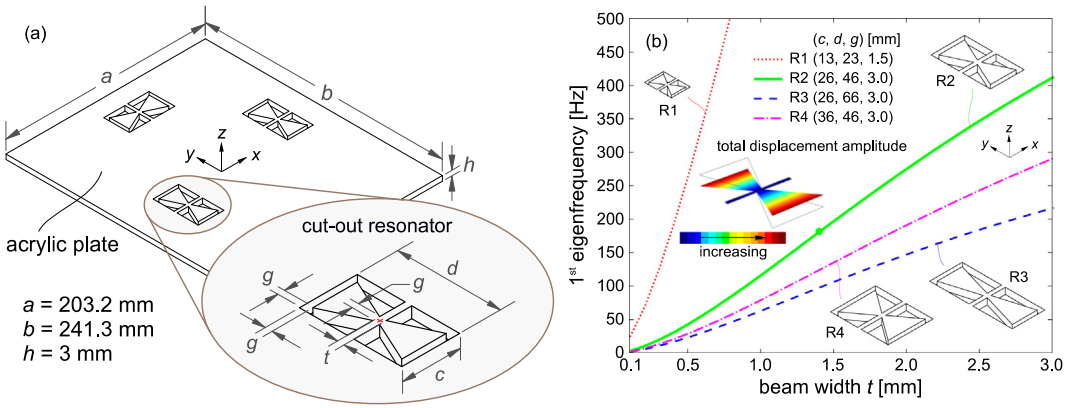

Fig. 1. (a) Schematic of host plate with cut-out resonators. (b) The first resonator eigenfrequency as a function of beam width for four resonators, with geometries shown in the insets. The inset is the first eigenmode shape of the resonator R2 with beam width of 1.4 mm.

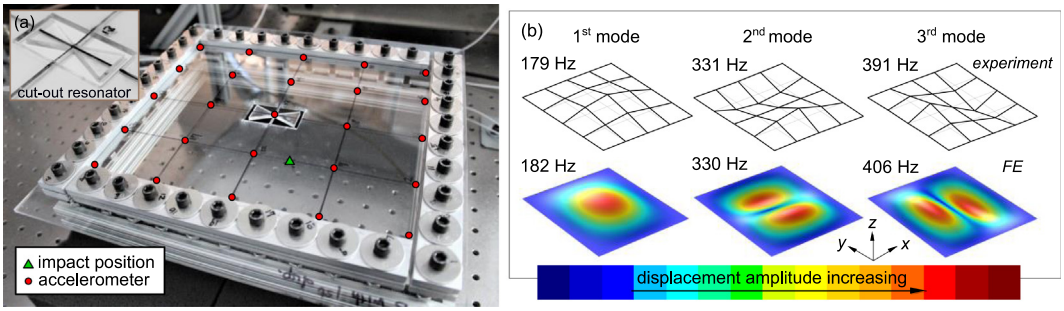

Fig. 2. (a) Photograph of clamped acrylic plate with a cut-out resonator. (b) Experimental and FE mode shapes of the clamped original plate for the three lowest modes.

Each experimental dataset involves the measurement of the 25 positions, which are highlighted by the red circle markers in Fig. 2(a). The Fourier transform of the exponentially windowed accelerometer time series is normalized by the Fourier transform of impact force, this spectral quantity is squared, and then averaged among all 25 data locations. By taking the square root of the resulting quantity, we obtain the global transfer function (TF) between the global acceleration and impact force. The experimental mode shapes of the original plate without cut-outs are reconstructed by extracting the imaginary part of the measurement positions at the experimentally determined natural frequencies. The top of Fig. 2(b) shows the experimental natural frequencies and corresponding mode shapes of the clamped original plate.

An FE model of the acrylic plate with width $a = 203.2$ mm, length $b = 241.3$ mm, and thickness $h = 3.0$ mm is created using shell elements in COMSOL Multiphysics. The four edges of the rectangular plate are fixed. The material properties used are the same as mentioned in Section 2. The natural frequencies and the corresponding mode shapes of clamped original plate for the three lowest modes determined by FE model are shown at the bottom of Fig. 2(b). The FE natural frequencies agree well with the experiments with absolute deviations less than 4%. In addition, a good agreement is observed between the FE and experimental mode shapes in Fig. 2(b). The results suggest that the experimental setup adequately reproduces the salient boundary conditions, material properties, and vibrating modes observed in the more idealized FE model.

Based on the validated FE model, simulations of the global TF frequency responses between the plate acceleration and input force are carried out. The input force is a unit point force in the z-direction to emulate the excitation method used in the experiments. The FE global TF response is calculated through the surface integration over the plate area of the acceleration amplitude in the z-direction, normalized by the unit point force. The following sections adopt these computational and experimental methods to explore the behaviors of the plate and cut-out resonators, and coupling amongst them.

4. Results and discussions

This section leverages integrated FE and experimental efforts to investigate the mechanisms leading to vibration attenuation in rectangular plates having cut-out resonators. The plates with resonators are classified by labels such as C1, S2, and F3. The characters C, S, and F respectively refer to the clamped plate, simply-supported plate, and freely-suspended plate. The numbers 1, 2, and 3 represent the plates respectively designed to mitigate the first, second, third modes of the plate vibration.

4.1. Clamped plate with cut-out resonators

Fig. 3(b, d) present the FE and experimental transfer functions (TFs) of the clamped original plate and plates C1, C1d, and C1r around the first plate mode. The latter three plates C1, C1d, and C1r employ the cut-out resonators R2 with dimensions $(c, d, g) = (26, 46, 3.0)$ mm. These dimensions are selected according to Fig. 1(b) to attenuate the first mode of plate vibration at 182 Hz. The resonator R2 corresponds to a coverage area of only 2.4% of the plate surface. Based on the rotational deformation of the first eigenmode shape in the inset of Fig. 1(b), the design concepts of the resonator location for best vibration attenuation are hypothesized: (1) positioning of the resonator at a location of a high bending moment gradient to offer a greater difference of internal shear forces applied to the two triangular masses to twist the central beam, (2) arranging the central beam along a nodal line of bending moment to subject the central beam to minimal internal shear force. Following the design concepts is hypothesized to lead to the most substantial attenuation of the plate dynamics around the first natural frequency due to the enhanced oscillation inclination of the cut-out resonators.

The contours of bending moments per unit length along x- and y-axis for the first mode of clamped original plate are shown in Fig. 3(a). There are four locations, including $(x, y) = (-0.29a, 0)$, $(0.29a, 0)$,

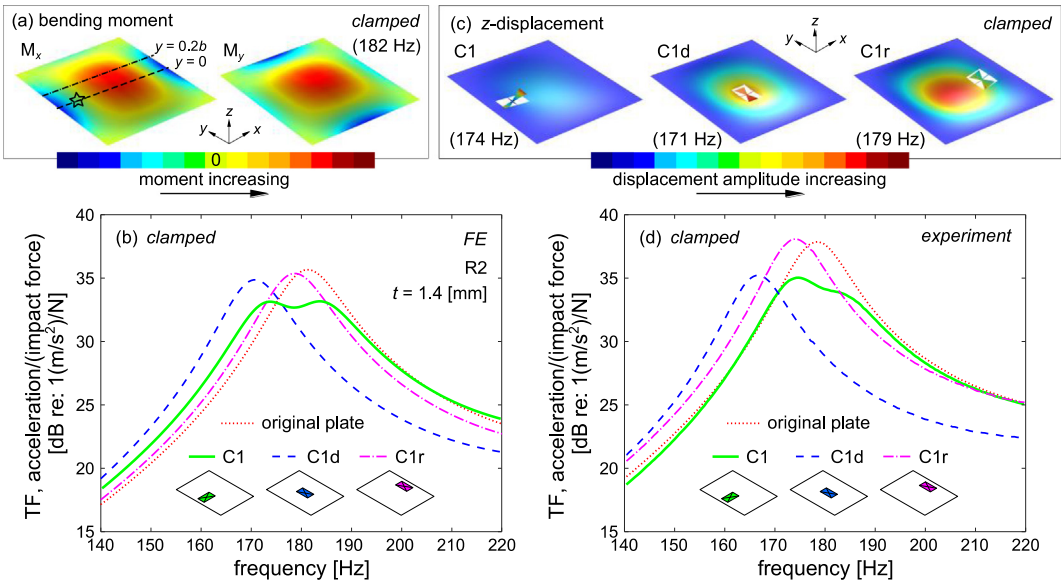

Fig. 3. (a) FE bending moment for the first mode of the clamped original plate. (b) FE and (d) experimental TF frequency responses of clamped plates without and with cut-out resonators at different locations around the first plate mode. (c) FE displacement contours of clamped plates with resonators R2 at different locations at the peak frequency of the first mode.

(0, −0.29*b*), and (0, 0.29*b*) with respect to the plate center, where the bending moment distribution mentioned above is able to excite the first resonator eigenmode. The location at (−0.29*a*, 0), highlighted by the star marker in Fig. 3(a), is selected to verify the operational principle of the cut-out resonator vibration attenuation for plate C1. For the plate C1d, the resonator is cut-out at the center of the plate (0, 0), which has maximum *z*-displacement amplitude at 182 Hz as seen in Fig. 2(b), a high bending moment amplitude, and near-zero bending moment gradient as seen in Fig. 3(a). The resonator of plate C1r is positioned at (0.29*a*, 0), which has zero bending moment and near-zero bending moment gradient along the length of resonator. The resonator locations and orientations for plates C1, C1d, and C1r are shown schematically in the insets of Fig. 3(b). The sizes of the resonators in the insets are exaggerated for ease of visualization. The impact force is applied at (−0.25*a*, −0.125*b*), the same as the impact position highlighted by green triangle marker in Fig. 2(a).

In Fig. 3(b), considering the plate C1 (green solid) with respect to original plate (red dotted), the FE TF peak amplitude decreases by 2.5 dB, and the peak frequency of the first mode shifts downwards by 4%. For the case with the cut-out resonator positioned at the plate center with maximum displacement amplitude, the first mode of plate C1d (blue dashed) has 0.8 dB peak amplitude attenuation, and a 6% lower resonant frequency compared with the original plate. The plate C1r (magenta dash–dot) shows only a reduction of 0.3 dB of peak TF amplitude with first mode frequency reduction of 1%. These trends are in good qualitative agreement with experiments reported in Fig. 3(d). In addition, compared with FE simulations, the plates C1 and C1d respectively have greater TF peak attenuations in experiments, 2.8 dB and 2.7 dB, than that observed for plate C1r.

The FE *z*-displacement contours of plate C1, C1d, and C1r for the first mode are shown in Fig. 3(c). For plate C1 in Fig. 3(c), the greatest deformations are in the resonators, and the plate vibrations are reduced. Unlike plate C1, the resonators in plates C1d and C1r are not greatly induced to vibrate due to the poor trigger of the resonator eigenmode. This explains the limited vibration attenuations achieved for the resonators in plates C1d and C1r. The greater vibration attenuation of plate C1 results from placement of the resonator at a location that provides high gradient of bending moment to twist the central beam and thus excite the first resonator eigenmode. The resonator in plate C1d is subjected to uniformly distributed internal shear forces, leading the entire resonator the uniformly displace, without means to trigger the first resonator eigenmode for vibration attenuation. For the resonator in plate C1r, the resonator is likewise subjected to uniformly distributed internal shear forces although the forces are near-zero in amplitude. Under the uniformly distributed loads, as seen in Fig. 3(c) the difference of displacements between two triangular masses of the resonator in plate C1r is relatively small. Hence, the first resonator eigenmode is not triggered to absorb plate vibration, resulting in almost no attenuation of the lowest order TF amplitude for plate C1r. This agrees with the principle observed for vibration absorbers by Anh et al. [42] and Cheung and Wong [11] whereby vibration absorbers are nonfunctional when forces are insufficiently applied near the attachment locations. The analogue in this research is the need for bending moment distribution at the placement of the cut-out resonators so that rotational trigger is achieved along the slender central beam driving the triangular masses.

To investigate how the bending moment distribution influences vibration suppression, the bending moment along *x*-axis for the first mode of the clamped original plate at y = 0 (dashed) and y = 0.2*b* (dash–dot) are retrieved from Fig. 3(a) and reported in Fig. 4(a). The plates C1h, C1o, and C1m are considered, and employ resonators R2 with beam width of 1.4 mm. The resonator location, bending moment along *x*-axis, and bending moment gradient $\partial M_x/\partial x$ for plates C1, C1h, C1o, and C1m are presented in Fig. 4(a). Based on the bending moment distribution on the clamped original plate shown in Fig. 4(a), the bending moments along the plate mid-plane perpendicular to the central beam of resonators in plates C1, C1h, C1o, and C1m are schematically shown in Fig. 4(b). Fig. 4(c) shows the FE TFs of the clamped original plate and plates C1, C1h, C1o, and C1m around the first plate mode. For plates C1 and C1m, the central beams of the resonators are arranged along a nodal line of bending moment, so that there is no net internal shear force applied to the central beams, as seen in Fig. 4(b). In Fig. 4(a), the bending moment gradient of the resonator location in plate C1m is 23.5 kN/m, which is lower than the case in plate C1, 33.7 kN/m. Compared to plate C1 (thick green solid) in Fig. 4(c), plate C1m (thin black solid) with a smaller bending moment gradient exhibits less peak TF amplitude attenuation using the same cut-out resonator as for plate C1. For these cases where the central beam of the resonator is oriented along a nodal line of bending moment, the resonator is subjected to a greater bending moment gradient to enhance trigger of the first resonator eigenmode with the plate dynamics for vibration suppression.

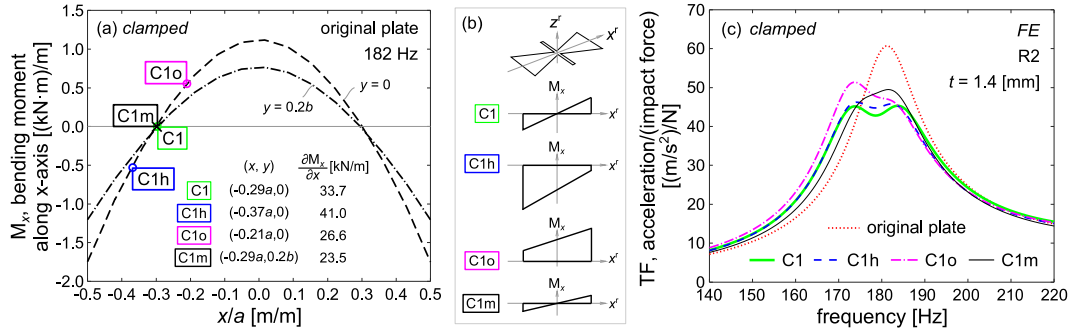

Fig. 4. (a) FE bending moment M_x for the first mode of the clamped original plate at y = 0 and y = 0.2*b*. (b) Schematics of bending moment on the line on the middle line perpendicular to the length of central beam of resonators in plates. (c) FE TF frequency responses of clamped plates without and with cut-out resonators at locations around the first plate mode.

Considering the case of having a great bending moment gradient without arranging the central beam along the nodal line of bending moment, plates C1h and C1o are selected, and the corresponding schematics are shown in Fig. 4(b). In Fig. 4(a), the central beam of the resonators for plates C1h and C1o are subjected to internal shear forces with amplitudes near 0.5 kN. The bending moment gradient at the resonator location in plate C1h is 41.0 kN/m, greater in value than the case for plate C1, 33.7 kN/m. Yet, less attenuation occurs of the plate vibration for plate C1h (blue dashed) in Fig. 4(c) compared to plate C1 (thick green solid). Similarly, plate C1o (magenta dash–dot) has less peak TF amplitude attenuation than plate C1m (thin black solid), although the bending moment gradient at the resonator location in plate C1o, 26.6 kN/m, is greater than the case in plate C1m, 23.5 kN/m. Together, these results indicate that even though the resonators for plates C1h and C1o are positioned at location providing greater bending moment gradient, there is less trigger of the first resonator eigenmode for vibration attenuation. This is because the central beam of the resonators in plates C1h and C1o are subjected to non-zero net internal shear forces, as shown in Fig. 4(b). The results suggest that minimal net internal shear force distribution on the central beam may excite the first resonator eigenmode. In addition to positioning at a location having a great bending moment gradient, arranging the central beam along the nodal line of bending moment is an influential approach to maximize the effectiveness of the cut-out resonators for plate vibration suppression.

4.2. Multi-mode triggering with cut-out resonators

To explore an extension of this vibration attenuation principle to higher order modes, Fig. 5(a, b) presents FE and experimental TF responses of the clamped original plate and plates denoted by C1, C2, C3, CT0 and CT at frequencies around the three lowest order plate modes. The T in the labels denotes that multiple resonators are employed to attenuate multiple modes of the host plate structure vibration. According to the design concept stated in Section 4.1, the resonators in plates C1, C2, and C3 are designed to mitigate the first, second, and third modes, respectively, of the clamped plate. The resonators R2 are therefore positioned at (−0.29*a*, 0), (0, 0.37*b*), and (0.37*a*, 0) with respect to the plate center. The beam widths of the resonators R2 in plate C1, C2, and C3 are respectively determined by the relationship between the eigenfrequency and beam width in Fig. 1(b) according to the first plate mode at 182 Hz, the second plate mode at 330 Hz, and the third plate mode at 406 Hz. The beam width values are given in Fig. 4(a). The three resonators in plates CT0 and CT designed for the first, second, and third modes and are each at the respective locations and orientations as chosen for the resonators in plates C1, C2, and C3. The three resonators in plate CT0 have the same beam widths as the corresponding beams in resonators placed for plates C1, C2, and C3. A plate having a greater number of cut-out resonators may possess less dynamic stiffness due to reduced material, which leads to lower natural frequencies. Consequently, for the plate CT, the resonators are designed with slightly smaller beam widths to accommodate the change in dynamic stiffness of the whole plate, whereas plate CT0 does not take this detail into account and utilizes resonators designed strictly according to Fig. 1(b).

Both FE and experimental TF frequency responses in Fig. 5(a, b) show that plates C1, C2, C3, CT0, and CT have vibration suppression around the designed modes. The FE and experimental peak TF attenuations for the three lowest modes of the plates are listed in Table 1. The FE peak attenuations of plate CT are 1.8 dB to 2.7 dB greater than for plate CT0. This confirms that the resonators in plate CT, which are designed according to the reduced dynamic stiffness of the plate due to the multiple resonators, induce greater vibration attenuation via more precise tuning and trigger. The plates with three cut-out resonators have slightly lower natural frequencies compared to plates with single resonator. For example, compared to the original plate, plates C1 with a single resonator and CT with three resonators have peak frequencies of the first mode shifted downward by 4% and 9%, respectively, from the original plate. The resonators with thinner beams in plate CT have lower resonator eigenfrequencies, which can meet the requirement to mitigate the plate modes at slightly lower natural frequencies. The plate CT with three cut-out resonators also have greater peak amplitude attenuations compared to the corresponding plates with single resonators in FE and experiments.

These results conclude that the cut-out resonators oscillate via triggering the first resonator eigenmodes to suppress plate global vibration levels. Although this concept has been explored with multiple modes of plate vibration, it has yet to be tested for other configurations of host plates and for other common implementations of vibration absorbing systems. These attributes are considered in the next Sections 4.3 and 4.4.

4.3. Cut-out resonator dimensions and number

Studies of vibration absorbers in lumped systems indicate that increasing the number of TMDs without changing the ratio of added mass can improve the effectiveness of the attached system to tailor and reduce the host structure dynamics [4,5,9,10,43]. To understand whether this approach applies to the cut-out resonators, resonators R1 are introduced and tuned according to the eigenfrequency relationship shown in Fig. 1(b). Fig. 6(a) presents the FE TF frequency responses of the clamped original plate and plates N1 and NT, where the N represents that the plate contains multiple cut-out resonators. The resonators used for plates N1 and NT are four cut-out resonators R1 with dimensions (*c*, *d*, *g*) = (13, 23, 1.5) mm. This corresponds to a coverage area of 2.4% for the set of resonators R1, which is the same area coverage as the single resonator R2. The beam widths of resonators R1 are selected according to Fig. 1(b) to attenuate the targeted first, second, and/or third mode of the plate, according to the plate label.

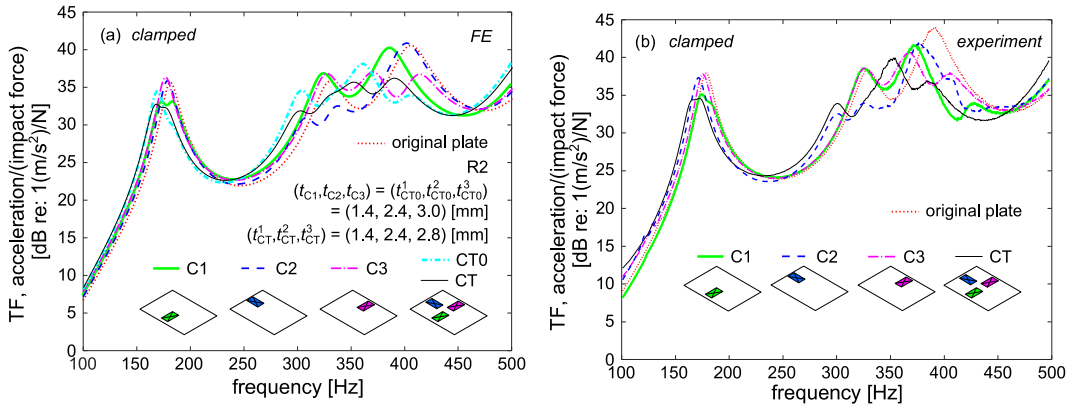

Fig. 5. (a) FE and (b) experimental TF frequency responses of clamped plates without and with cut-out resonators R2. The resonators in plates C1, C2, and C3 are designed to mitigate the first, second, and three modes of the clamped plate vibration, respectively. The resonators in plates CT0 and CT are designed to mitigate the three lowest modes of vibration.

Table 1
FE and experimental TF peak amplitude attenuations for the three lowest modes of clamped plates with cut-out resonators R2.

Clamped plate	FE (plate notation), experiment (plate notation)	
	Single resonator	Three resonators
1st mode	2.5 dB (C1), 2.8 dB (C1)	1.1 dB (CT0), 2.9 dB (CT), 3.3 dB (CT)
2nd mode	3.4 dB (C2), 4.4 dB (C2)	1.2 dB (CT0), 3.9 dB (CT), 4.5 dB (CT)
3rd mode	3.5 dB (C3), 3.2 dB (C3)	2.5 dB (CT0), 4.4 dB (CT), 3.4 dB (CT)

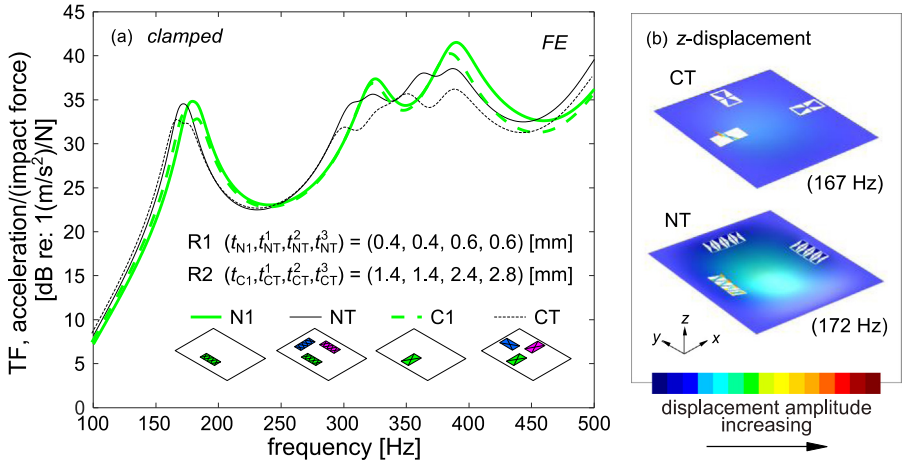

Fig. 6. (a) FE TF frequency responses of clamped plates with cut-out resonators. The resonators in plates N1 and NT are R1, and resonators in plates C1 and CT are R2. The plates C1 and N1 are designed to mitigate the first mode, and plates CT and NT are designed for the three lowest modes of the clamped plate vibration. (b) FE displacement contours of plates CT and NT at the peak frequency of the first modes.. (For interpretation of the references to color in this figure legend, the reader is referred to the web version of this article.)

The sets of resonators in plates N1 and NT are positioned at the same locations and orientations as the plates C1 and CT, respectively.

Considering the FE results of plates designed to mitigate the first mode in Fig. 6(a), the peak amplitude attenuations of plates N1 is 1.5 dB less than plate C1. The FE peak amplitude attenuations of plate NT for the first, second, and third modes are respectively 1.8 dB, 3.7 dB, and 2.4 dB, less than plate CT. The results indicate that sets of small-size cut-out resonators may be less effective at vibration suppression than the resonators with the same area coverage, which is counter-intuitive with respect to the findings in previous studies [4,5,9,10]. Considering the influences of resonator location on plate vibration suppression, vibration absorbers are less functional when there are no sufficient forces applied to the location of vibration absorbers [11,34,42]. As seen in Fig. 3(a) for the first mode, the locations of the resonator R2 and the set of resonators R1 are positioned at the star marker, $(-0.29a, 0)$. The shorter length of the triangular masses for resonators R1 results in inadequate momentum to excite the first resonator eigenmode as greater as for resonator R2. In addition, the moment of inertia of the cut-out resonator R1 may also influence the trigger of the first resonator eigenmode. Compared to resonator R2, resonator R1 has a smaller radius of gyration, thus leading to a smaller moment of inertia about the central beam, and thus less net inertia to contribute to the vibration attenuation. Together, the findings suggest that utilizing cut-out resonators for plate vibration attenuation is more successful with greater lumped inertia in the resonators than distributed inertia.

The FE z-displacement contours of plates CT and NT for the lowest modes are shown in Fig. 6(b). For plate CT with resonators R2 at 167 Hz, the greatest deformations are in the resonator at $(-0.29a, 0)$, highlighted by green in the insets of Fig. 6(a), while the plate vibration is reduced. The set of resonators at $(-0.29a, 0)$ in plate NT designed to mitigate the first plate mode are excited simultaneously at 172 Hz in Fig. 6(b). Yet, the plate NT remains the similar displacement

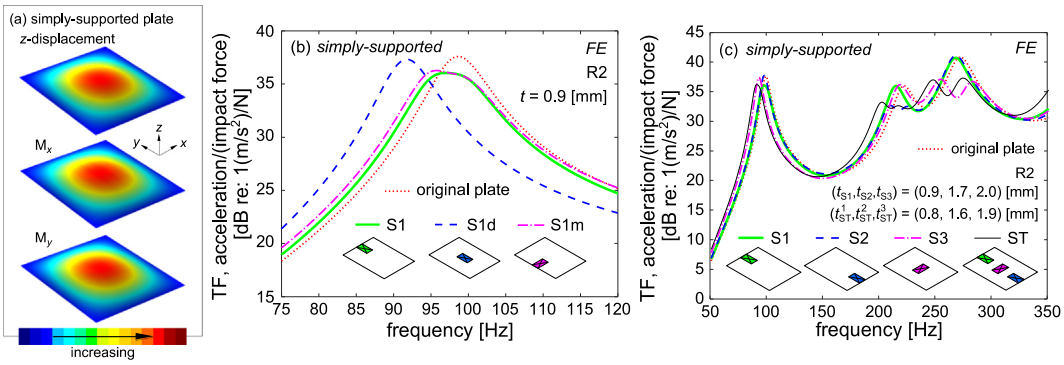

Fig. 7. (a) Displacement and bending moment contours for the first mode of simply-supported original plate at 98 Hz. (b) TF frequency responses of simply-supported plates without and with a cut-out resonator at various locations around the first plate mode. (c) TF frequency responses of simply-supported plates without and with resonators at frequencies around the three lowest modes. The resonators in plates S1, S2, S3, and ST are designed to mitigate the first, second, three, and the three lowest modes of the simply-supported plate vibration, respectively.

distribution as the first mode of original plate as seen in Fig. 2(b). The result implies the vibration suppression is limited for the plate employing the cut-out resonator with a short length of the triangular masses.

4.4. Extensibility of resonant working principle to other plate boundary conditions

The working principle of the cut-out resonator is to oscillate the first resonator eigenmode. To trigger the first resonator eigenmode for vibration suppression, the resonator is positioned at the location offering a great bending moment gradient so that the central beam is oriented along the nodal line of bending moment. Yet, there are certain modes having the nodal line of bending moment on the edge of the plate, such as the first mode of simply-supported plate and the second mode of freely-suspended plate, so that these modes may not have a location that can meet the design concept of arranging the central beam. To understand how to excite the cut-out resonators with other common plate boundary conditions, this section examines the vibration attenuation of cut-out resonators in simply-supported and freely-suspended plates.

Fig. 7(a) presents the contours of z-displacement and bending moments along x- and y-axis for the first mode of a simply-supported original plate. The bending moment nodal lines occurs on the four edges of the plate, and high gradient of bending moment is precisely at the four edges of the simply-supported plate. Although there is no location for which the central beam of a cut-out resonator may be positioned along a nodal line of bending moment, the resonator may be positioned at the location offering a sufficiently large bending moment gradient to trigger the first resonator eigenmode for vibration attenuation. To study how the bending moment gradient influences the vibration suppression of simply-supported plates, the forced vibrations of plates S1, S1d, and S1m around the first mode are examined by FE simulations. The resonators in the three plates are resonators R2 with beam width of 0.9 mm, determined by the relationship between the first eigenfrequency and beam width in Fig. 1(b) based on the first mode of simply-supported plate at 98 Hz. The resonators in plates S1 and S1m are respectively positioned at $(0,\ 0.5b-0.5d-g)$ and $(-0.5a+0.5d+g,\ 0)$, near to the bending moment nodal lines, so as to provide a high bending moment gradient as seen in Fig. 7(a). The resonator in plate S1d it located at the plate center (0, 0), the location with maximum z-displacement amplitude, high bending moment amplitude, and near-zero bending moment gradient in Fig. 7(a). The impact force is applied at $(-0.25a,\ -0.125b)$.

The TF frequency responses of simply-supported original plate and plates S1, S1d, and S1m at frequencies around the three lowest modes are presented in Fig. 7(b). The first modes of plates S1, S1d, and S1m respectively have 1.6 dB, 0.3 dB, and 1.3 dB peak amplitude attenuation and 2%, 7%, and 3% lower resonant frequency compared with the original plate. Even though the central beam is not arranged along the nodal line of bending moment, the positioning of resonators at locations of high gradient of bending moment, such as for plates S1 and S1m, leads to greater attenuation than when the cut-out resonators are located near small bending moment gradients, like for plate S1d. This is because a high bending moment gradient offers a sufficient difference between the internal shear forces applied to the two triangular masses inducing twist and activation of the first resonator eigenmode. Thus, even without means to arrange the central beam along the bending moment nodal line, positioning cut-out resonators at a location providing a high bending moment gradient may still induce targeted vibration suppression.

Table 2
TF peak amplitude attenuations for the three lowest modes of simply-supported plates with cut-out resonators R2.

Simply-supported plate	Single resonator (plate notation)	Three resonators (plate notation)
1st mode	1.6 dB (S1)	1.4 dB (ST)
2nd mode	3.3 dB (S2)	2.8 dB (ST)
3rd mode	3.7 dB (S3)	3.5 dB (ST)

The TF frequency responses of the simply-supported original plate and plates S1, S2, S3, and ST at frequencies around the three lowest modes are presented in Fig. 7(c). The resonators in plates S1, S2, S3, and ST are resonators R2, with beam widths determined based on the relations between the first resonator eigenfrequency and beam width in Fig. 1(b) tuned to suppress corresponding plate resonances. The locations of resonators in plates S1, S2, and S3 are $(0,\ 0.5b-0.5d-g)$, $(0,\ -0.5b+0.5d+g)$, and (0, 0), respectively. For plate ST, the resonators are positioned at the same locations with the same orientations as the plates S1, S2, and S3. As expected, plates S1, S2, S3, and ST respectively have vibration suppressions around the first, second, third, and the three lowest modes. Table 2 lists the TF peak amplitude attenuations for the three lowest modes of simply-supported plates with cut-out resonators. The results suggest the resonator can be utilized for vibration suppression of simply-supported plates.

Fig. 8 presents the TF frequency responses of the freely-suspended original plate and plates F1, F2, F3, and FT at frequencies around the three lowest order modes. The plates F1, F2, F3, and FT utilize cut-out resonators R2. The beam widths of the resonators are determined by the relation between the first resonator eigenfrequency and beam width in Fig. 1(b) according to the frequencies the resonator eigenmodes are designed to mitigate. The resonators in plates F1, F2, and F3 are respectively positioned at $(-0.5a+0.5c+g,\ 0)$, $(0,\ 0.5b-0.5d-g)$, and $(0.5a-0.5d-g,\ 0)$. For plate ST, the locations and orientations of resonators are the same as plates F1, F2, and F3. The impact force is

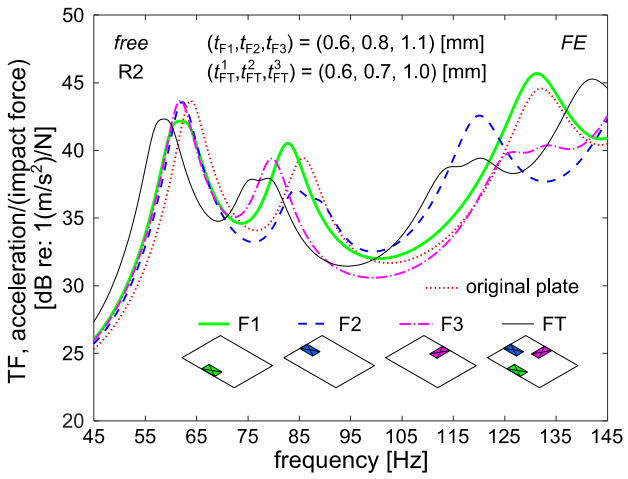

Fig. 8. TF frequency responses of freely-suspended plates without and with cut-out resonators. The resonators in plates F1, F2, F3, and FT are respectively designed to mitigate the first, second, three, and the three lowest modes of the freely-suspended plate vibration.

Table 3
TF peak amplitude attenuations for the three lowest modes of freely-suspended plates with cut-out resonators R2.

Freely-suspended plate	Single resonator (plate notation)	Three resonators (plate notation)
1st mode	1.5 dB (F1)	1.3 dB (FT)
2nd mode	2.3 dB (F2)	1.5 dB (FT)
3rd mode	4.2 dB (F3)	5.1 dB (FT)

applied at $(-0.5a, -0.5b)$. The plates F1, F2, F3, and FT respectively reveal vibration suppression around the first, second, third, and the three lowest modes as expected. The TF peak amplitude attenuations for the three lowest modes of freely-suspended plates with cut-out resonators are listed in Table 3. The third modes have greater vibration suppression than the first and second modes. The peak amplitude attenuation increases with the increasing frequency of the attenuating mode, which is also observed for FE clamped plates, simply-supported plates, and freely-suspended plates with resonators. The results reveal that the cut-out resonators are more effective for the higher order modes in vibration suppression in these comparisons.

4.5. Perspectives on exploiting cut-out resonators for tuned vibration absorption

This research finds that designing the cut-out shapes for lowest order modal response, positioning the cut-outs near locations offering a high bending moment gradient so that the central resonator beam is colinear with a nodal line of plate bending moment best excites the first resonator eigenmode for host plate vibration suppression. This principle is directly extensible to other plate boundary conditions since the mechanism needed to trigger the resonator eigenmode is independent of the plate boundary. Furthermore, the resonator only covers a small surface area, while the resonator mass is simply a small proportion of host structure mass so that there is no attachment on the panel. This practice of thin plate design and cut-outs for intrinsic vibration suppression has a wide variety of implementations for diverse engineering applications, ranging from vehicle panels with inherent radiated noise control, to lightweight and 'damped' machine covers without need for particular damping materials, and beyond.

On the other hand, this resonator implementation may have limitations including an indirect influence on plate mechanical capabilities, ultimate attenuation performance and durability. In other words, by introducing the cut-outs to the plate, the mechanical stiffness and load-bearing ability of the plate may be adversely affected. Yet, there are numerous applications for which non-load-bearing plates are required, such as panels used for noise control or aerodynamics, justifying the outcomes of this report for sake of those engineering systems. Compared to an approach of attaching vibration absorbing resonators [35–37], the cut-out resonator has a modest attenuation especially at the lowest order mode due to relatively small resonator mass compared to the remaining plate modal mass. The slender central beam of the resonator may also be susceptible to failure when resonating over a long operational life, especially when the beam width is thinner than the plate thickness.

To enhance the vibration attenuation capabilities, a direct method is to utilize larger size cut-out resonators. As shown in Fig. 1(b), using the larger size resonator R3 for a constant frequency, the central beam is wider than the small size resonator R2, and it can provide greater resonator mass. Fig. 9(b) presents the FE TF frequency responses of the clamped original plate and plate C1g around the first plate mode. The plate C1g utilizes resonator R3 with beam width of 2.5 mm, which is around 80% of the plate thickness. The results show that peak attenuations of plate C1g is 3.9 dB, which is greater than plate C1, 2.5 dB. Together, this method can improve the attenuation performance by increasing resonator mass, although it may both increase the require surface area coverage committed to the resonators and may reduce mechanical performance of a load-bearing host plate.

To improve the durability of the cut-out resonators, a small coating of elastomer may be applied on the rotating central beam to act like an unconstrained free layer damping that limits the peak displacement of the cut-out. Fig. 9(a) shows the lowest order mode eigenfrequencies for resonators R2 and R2s as a function of the acrylic beam width. Resonator R2s introduces a thin coating of silicone rubber to the exposed, rotating beams of resonator R2, with rubber width s and thickness h, as shown in the inset of Fig. 9(a). The material properties of the silicone rubber are: Young's modulus 200 kPa, density 1145 kg/m^3, Poisson's ratio 0.49, and structural loss factor 0.2 [37]. The deviations of the first resonator eigenfrequencies between R2 and R2s are less than 4%. Due to the similar first eigenfrequencies, plate C1s uses resonators R2s with the same positions and beam width as the resonators R2 in plate C1. Fig. 9(b) presents the FE TF frequency responses of clamped original plate and plates C1 and C1s around the first plate mode. As expected, plate C1s has vibration suppression around the first mode similar to the response of plate C1, showing that the incorporation of the silicone rubber does not deter the vibration attenuation performance of the cut-out resonator. The results suggest that a thin coating of elastomer over the cut-out resonator beams could assist to prolong working life of the resonators without adversely affecting the vibration suppression capability.

Overall, the resonator using only a small proportion of the plate area is found to attenuate plate vibration by exciting the first resonator eigenmodes, which couple to the bending moments of the place. This concept is moreover extensible to any plate boundary condition combination. Although the cutout design may have the limitations of attenuation performance and durability, these may resolved by a variety of methods. The resonator design may also provide the multiple functions of cutouts for accommodating mountings and accessories in engineering applications.

5. Conclusions

This research investigates the mechanisms of plate vibration attenuation for cut-out resonators. Via FE and experimental efforts, the studies reveal that embedding the resonators at locations offering high bending moment gradient and arranging the central resonator beam along a nodal line of bending moment can best excite the first resonator eigenmode. As a result, maximum vibration attenuation occurs by exploiting these design conditions. Moreover, this design principle is extensible

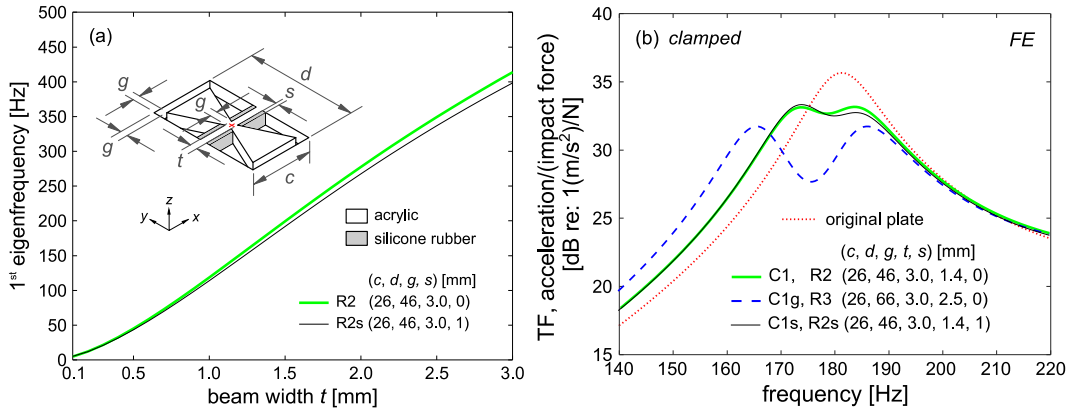

Fig. 9. (a) The first resonator eigenfrequency as a function of acrylic beam width for resonators with and without widening central beam by silicone rubber. (b) FE TF frequency responses of clamped plates with cut-out resonators. The resonator in plate C1, C1g, and C1s are R2, R3, and R2s, respectively. Plates C1, C1g, and C1s are designed for the first modes of the clamped plate vibration.

to any plate boundary conditions due to the underlying principle tied solely to structural vibrations that is independent of boundaries. These design concepts, rules, and findings may guide the development of cut-out resonators for vibration suppression of plates with arbitrary boundary.

CRediT authorship contribution statement

Sih-Ling Yeh: Conceived the ideas of the research, Carried out the theoretical and experimental research efforts, Analyzed the data and processed conclusions, Edited the manuscript. **Ryan L. Harne:** Conceived the ideas of the research, Analyzed the data and processed conclusions, Edited the manuscript.

Declaration of competing interest

The authors declare that they have no known competing financial interests or personal relationships that could have appeared to influence the work reported in this paper.

Acknowledgments

This project is supported by the National Science Foundation, United States Faculty Early Career Development Award (No. 2054970).

References

[1] S. Krenk, Frequency analysis of the tuned mass damper, J. Appl. Mech. 72 (2005) 936–942.
[2] M.Z. Ren, A variant design of the dynamic vibration absorber, J. Sound Vib. 245 (2001) 762–770.
[3] Y. Shen, H. Peng, X. Li, S. Yang, Analytically optimal parameters of dynamic vibration absorber with negative stiffness, Mech. Syst. Signal Process. 85 (2017) 193–203.
[4] A.S. Joshi, R.S. Jangid, Optimum parameters of multiple tuned mass dampers for base-excited damped systems, J. Sound Vib. 202 (1997) 657–667.
[5] L. Zuo, Effective and robust vibration control using series multiple tuned-mass dampers, J. Vib. Acoust. 131 (2009) 031003.
[6] H.N. Li, X.L. Ni, Optimization of non-uniformly distributed multiple tuned mass damper, J. Sound Vib. 308 (2007) 80–97.
[7] W.O. Wong, Y.L. Cheung, Optimal design of a damped dynamic vibration absorber for vibration control of structure excited by ground motion, Eng. Struct. 30 (2008) 282–286.
[8] Y. Shen, Z. Xing, S. Yang, J. Sun, Parameters optimization for a novel dynamic vibration absorber, Mech. Syst. Signal Process. 133 (2019) 106282.
[9] K.K. Reichl, D.J. Inman, Lumped mass model of a 1d metastructure for vibration suppression with no additional mass, J. Sound Vib. 403 (2017) 75–89.
[10] T. Igusa, K. Xu, Vibration control using multiple tuned mass dampers, J. Sound Vib. 175 (1994) 491–503.
[11] Y.L. Cheung, W.O. Wong, H∞ and H2 optimizations of a dynamic vibration absorber for suppressing vibrations in plates, J. Sound Vib. 320 (2009) 29–42.
[12] C.K. Hui, C.F. Ng, Autoparametric vibration absorber effect to reduce the first symmetric mode vibration of a curved beam/panel, J. Sound Vib. 330 (2011) 4551–4573.
[13] H. Peng, P.F. Pai, Acoustic metamaterial plates for elastic wave absorption and structural vibration suppression, Int. J. Mech. Sci. 89 (2014) 350–361.
[14] X.W. Yang, J.S. Lee, Y.Y. Kim, Effective mass density based topology optimization of locally resonant acoustic metamaterials for bandgap maximization, J. Sound Vib. 383 (2016) 89–107.
[15] Z. Wang, Q. Zhang, K. Zhang, G. Hu, Tunable digital metamaterial for broadband vibration isolation at low frequency, Adv. Mater. 28 (2016) 9857–9861.
[16] C. Sugino, Y. Xia, S. Leadenham, M. Ruzzene, A. Erturk, A general theory for bandgap estimation in locally resonant metastructures, J. Sound Vib. 406 (2017) 104–123.
[17] H. Peng, P.F. Pai, H. Deng, Acoustic multi-stopband metamaterial plates design for broadband elastic wave absorption and vibration suppression, Int. J. Mech. Sci. 103 (2015) 104–114.
[18] C. Gao, D. Halim, X. Yi, Study of bandgap property of a bilayer membrane-type metamaterial applied on a thin plate, Int. J. Mech. Sci. 184 (2020) 105708.
[19] M. Oudich, M. Senesi, M.B. Assouar, M. Ruzenne, J.H. Sun, B. Vincent, Z. Hou, T.T. Wu, Experimental evidence of locally resonant sonic band gap in two-dimensional phononic stubbed plates, Phys. Rev. B 84 (2011) 165136.
[20] M.B. Assouar, J.H. Sun, F.S. Lin, J.C. Hsu, Hybrid phononic crystal plates for lowering and widening acoustic band gaps, Ultrasonics 54 (2014) 2159–2164.
[21] Y. Huang, J. Li, W. Chen, R. Bao, Tunable bandgaps in soft phononic plates with spring-mass-like resonators, Int. J. Mech. Sci. 151 (2019) 300–313.
[22] J.C. Hsu, T.T. Wu, Lamb waves in binary locally resonant phononic plates with two-dimensional lattices, Appl. Phys. Lett. 90 (2007) 201904.
[23] T. Yu, G.A. Lesieutre, Damping of sandwich panels via three-dimensional manufactured multimode metamaterial core, AIAA J. 55 (2017) 1440–1449.
[24] D. Beli, J.R.F. Arruda, M. Ruzzene, Wave propagation in elastic metamaterial beams and plates with interconnected resonators, Int. J. Solids Struct. 139 (2018) 105–120.
[25] Y. Jin, Y. Shi, G.C. Yu, G.T. Wei, B. Hu, L.Z. Wu, A multifunctional honeycomb metastructure for vibration suppression, Int. J. Mech. Sci. 188 (2020) 105964.
[26] M. Nouh, O. Aldraihem, A. Baz, Wave propagation in metamaterial plates with periodic local resonances, J. Sound Vib. 341 (2015) 53–73.
[27] J. Jung, H.G. Kim, S. Goo, K.J. Chang, S. Wang, Realisation of a locally resonant metamaterial on the automobile panel structure to reduce noise radiation, Mech. Syst. Signal Process. 122 (2019) 206–231.
[28] W. Kuang, Z. Hou, Y. Liu, He effects of shapes and symmetries of scatterers on the phononic band gap in 2D phononic crystals, Phys. Lett. A 332 (2004) 481–490.
[29] Y.Z. Wang, F.M. Li, K. Kishimoto, Y.S. Wang, W.H. Huang, Elastic wave band gaps in magnetoelectroelastic phononic crystals, Wave Motion 46 (2009) 47–56.
[30] L. Marian, A. Giaralis, Optimal design of a novel tuned mass-damper–inerter (TMDI) passive vibration control configuration for stochastically support-excited structural systems, Probab. Eng. Mech. 38 (2014) 156–164.
[31] I.F. Lazar, S.A. Neild, D.J. Wagg, Using an inerter-based device for structural vibration suppression, Earthq. Eng. Struct. Dyn. 43 (2014) 1129–1147.
[32] Y. Shen, L. Chen, X. Yang, D. Shi, J. Yang, Improved design of dynamic vibration absorber by using the inerter and its application in vehicle suspension, J. Sound Vib. 361 (2016) 148–158.
[33] J.F. Toftekær, A. Benjeddou, J. Høgsberg, S. Krenk, Optimal piezoelectric resistive-inductive shunt damping of plates with residual mode correction, J. Intell. Mater. Syst. Struct. 29 (2018) 3346–3370.
[34] J. Plattenburg, J.T. Dreyer, R. Singh, Vibration control of a cylindrical shell with concurrent active piezoelectric patches and passive cardboard liner, Mech. Syst. Signal Process. 91 (2017) 422–437.

[35] L. Sun, Experimental investigation of vibration damper composed of acoustic metamaterials, Appl. Acoust. 119 (2017) 101–107.
[36] K.Y. Au-Yeung, B. Yang, L. Sun, K. Bai, Z. Yang, Super damping of mechanical vibrations, Sci. Rep. 9 (2019) 1–10.
[37] S.L. Yeh, R.L. Harne, Structurally-integrated resonators for broadband panel vibration suppression, Smart Mater. Struct. 29 (2020) 085010.
[38] P. Gao, A. Climente, J. Sánchez-Dehesa, L. Wu, Single-phase metamaterial plates for broadband vibration suppression at low frequencies, J. Sound Vib. 444 (2019) 108–126.
[39] H. Al Ba'ba'a, M.A. Attarzadeh, M. Nouh, Experimental evaluation of structural intensity in two-dimensional plate-type locally resonant elastic metamaterials, J. Appl. Mech. 85 (2018) 041005.
[40] H.W. Dong, S.D. Zhao, Y.S. Wang, C. Zhang, Topology optimization of anisotropic broadband double-negative elastic metamaterials, J. Mech. Phys. Solids 105 (2017) 54–80.
[41] M.H. Ulz, S.E. Semercigil, Vibration control for plate-like structures using strategic cut-outs, J. Sound Vib. 309 (2008) 246–261.
[42] N.D. Anh, H. Matsuhisa, L.D. Viet, M. Yasuda, Vibration control of an inverted pendulum type structure by passive mass–spring-pendulum dynamic vibration absorber, J. Sound Vib. 307 (2007) 187–201.
[43] J.F. Vignola, J.A. Judge, A.J. Kurdila, Shaping of a system's frequency response using an array of subordinate oscillators, J. Acoust. Soc. Am. 126 (2009) 129–139.